

3. Amundsen-Scott South Pole Station (9/16/22–3/29/23)

This report describes quality control of solar data recorded at Amundsen-Scott South Pole Station between 9/16/22 and 3/29/23. The period resulted in a total of 12,928 solar scans from the SUV-100 spectroradiometer, which were assigned to Volume 32. There was no site visit by NOAA personnel during this period. As in the past, the accuracy of solar data from the SUV-100 system was assured based on comparisons with measurements of the station's GUV-541 radiometer plus results of radiative transfer model calculation. The latter are part of the SUV-100's Version 2 dataset.

The sensitivity of the system was extraordinary stable over the reporting period; only one calibration file was required. However, the wavelength stability of the SUV-100 monochromator was degraded as in the last years, requiring frequent adjustment of the system's wavelength registration during post-processing.

After a "major" upgrade of the Windows 10 Operating System on 1/3/22, communication between the system's control computer and peripheral electronics slowed down considerably. As a consequence, spectral scans lasted longer than 15 minutes and the standard schedule of four scans per hour could no longer be maintained. Instead, measurements were performed on top of the hour and at 20 and 40 minutes past the hour. The problem was corrected on 2/3/23 when the serial port adapter that is integral to the computer was replaced with a modern USB-to-serial adapter. From 2/7/23 onward, the system is now again performing four scans per hour.

Since 2014, measurements of the 320 nm channel of the GUV-541 radiometer (S/N 29239) that is installed next to the SUV-100 spectroradiometer drifted greatly. GUV data products had to be produced without utilizing measurements of this channel. A comparison of calibrated GUV and SUV data performed during the Volume 26 season indicated that the quality of GUV data products is only marginally affected by the omission of the 320 nm channel. Solar data of the GUV are therefore part of the published datasets.

The system's PSP radiometer was installed during the site visit in January 2020. Its serial number is 27228F3 and it has a calibration factor of $8.332 \times 10^{-6} \text{ V}/(\text{W m}^{-2})$.

3.1. Irradiance Calibration

The on-site irradiance standards used for calibrating the SUV-100 spectroradiometer during the reporting period were the lamps M-666, 200W021, 200W013, 200WN005 and 200WN006. Lamps M-666, 200W021, and 200W013 are "working standards," which are used on a regular basis. Please see previous Operations Reports on the history of these lamps. Lamps 200WN005 and 200WN006 were left at the South Pole in March 2014. Both lamps are designated "long-term" standards and are typically only used during site visits. Both lamps were calibrated by CUCF in August 2013 (see below). Lamp 200WN005 was used both at the start and end of the reporting period while lamp 200WN006 was used only at the end.

Comparisons of calibrations with the various lamps suggested that the brightness of lamp 200W013 fluctuated over the reporting period. Similar fluctuations have been observed also during the last three seasons. Hence, absolute scans of the lamp were not used for the preparation of solar data.

Calibration history of long-term standards

The long-term standards 200WN005 and 200WN006 were calibrated against lamps 200WN001 and 200WN002 on 8/20/13. Lamps 200WN001 and 200WN002 had in turn been calibrated by Biospherical Instruments in November 2012 against the NIST standard F-616 using a multi-filter transfer radiometer. NIST standard F-616 is traceable to the detector-based scale of irradiance established by NIST in 2000. At the time lamps 200WN001 and 200WN002 were calibrated, they were also compared with the long-term traveling standard 200W017 of the NSF UV monitoring network. The irradiance scales of NIST standard F-616 and lamp 200W017 agreed to within 0.3%.

In early 2020, the chain of calibrations applied to solar data of the NSF and NOAA monitoring networks between 1996 and 2019 was re-evaluated (Bernhard and Stierle, 2020). This analysis suggested that the scale of spectral irradiance of NIST standard F-616 is low compared to the scale of primary standards used before 2013. This bias is -2% at 300 nm, -1% at 375 nm, and less than $\pm 0.5\%$ between 420 and 600 nm. **Version 2 solar data of Volume 29–32 were scaled upward accordingly, however, Version 0 data of these volumes remain traceable to the original scale of the primary standard F-616.**

Figure 2 shows a comparison of the working standards and the long-term standard 200WN005 based on absolute scans performed on 9/10/22, shortly before the commencement of solar measurements at the South Pole. The scales of spectral irradiance of lamps M-666, 200W021, and 200WN005 agree to within $\pm 1\%$ while the scale of lamp 200W013 differs by 2.5% from the average scale of the other lamps. As noted above, lamp 200W013 is unstable and was not used for calibrating solar data. The difference of $\pm 1\%$ for the other lamps is within the combined uncertainty of the scales of the these lamps.

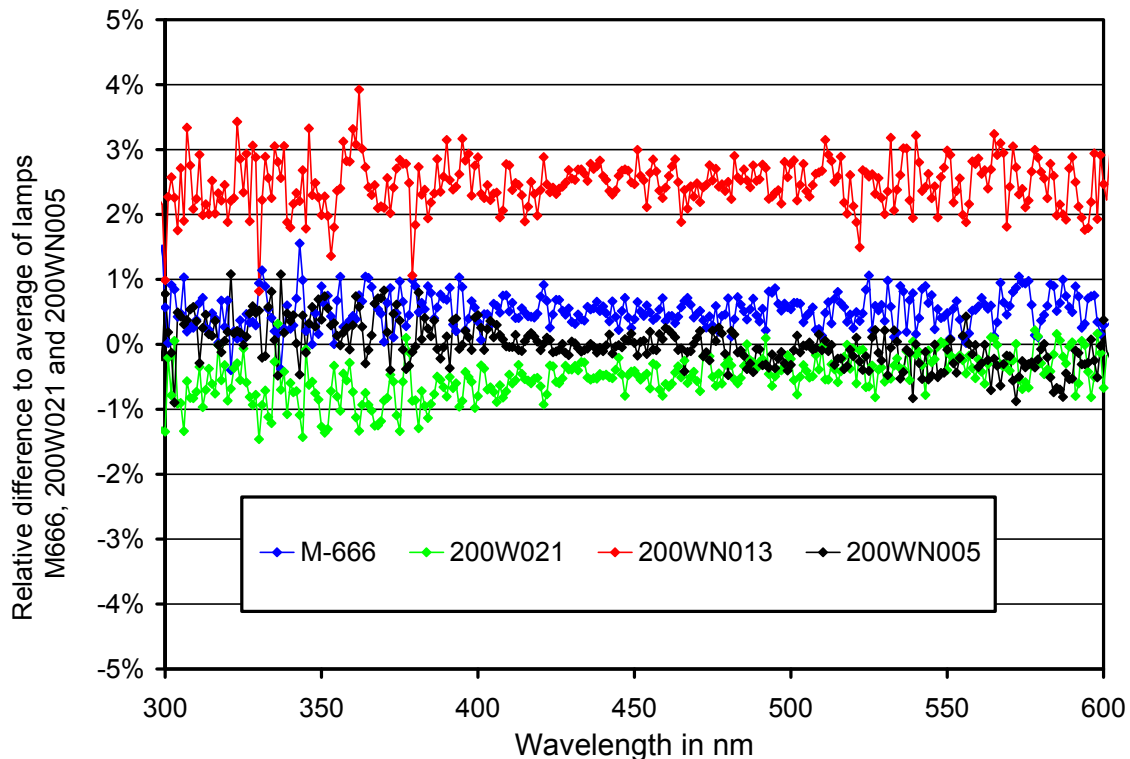


Figure 1. Comparison of South Pole working standard M-666, 200W021, and 200WN013 with long-term standard 200WN005 calculated from calibration scans performed on 9/10/22.

The GUV-541 radiometers was calibrated vicariously against SUV-100 Version 0 data. Calibration factors were established in the same way as those of previous volumes. Calibration factors of the last six years (Volumes 23 –32) agree to within $\pm 1.4\%$ ($\pm 1\sigma$) for all GUV channels, with exception of the drifting 320 nm channel. This result confirms the good consistency of calibrations over time.

3.2. Instrument Stability

The temporal stability of the spectroradiometer’s sensitivity was assessed with (1) bi-weekly calibrations utilizing the on-site standards, (2) daily “response” scans of the internal irradiance reference lamp, (3) comparison with data of the collocated GUV-541 radiometer, and (iv) model calculations, which are part of the “Version 2” data edition (Bernhard et al., 2004).

The internal reference lamp is monitored with a filtered photodiode with sensitivity in the UV-A range, called “TSI”. This photodiode has proven to be very stable over time and its measurements therefore allow to decouple temporal drifts of the internal lamp from changes in the SUV-100’s responsivity. These changes may be caused by variations in monochromator throughput or PMT sensitivity. Figure 2 shows changes in TSI readings and PMT currents at 300 and 400 nm, which were derived from the daily scans of the internal lamp during the reporting period. TSI measurements steadily decreased by about 1.2% during the reporting period, indicating some dimming of the internal reference lamp. PMT currents at 300 and 400 nm also showed a downward trend in response to the change in the lamp’s output but their variability is larger than that of the TSI data. The change in PMT currents during the last month of the reporting period is also somewhat larger than that of the TSI measurement. The magnitude of these variations is within the normal range observed in previous years.

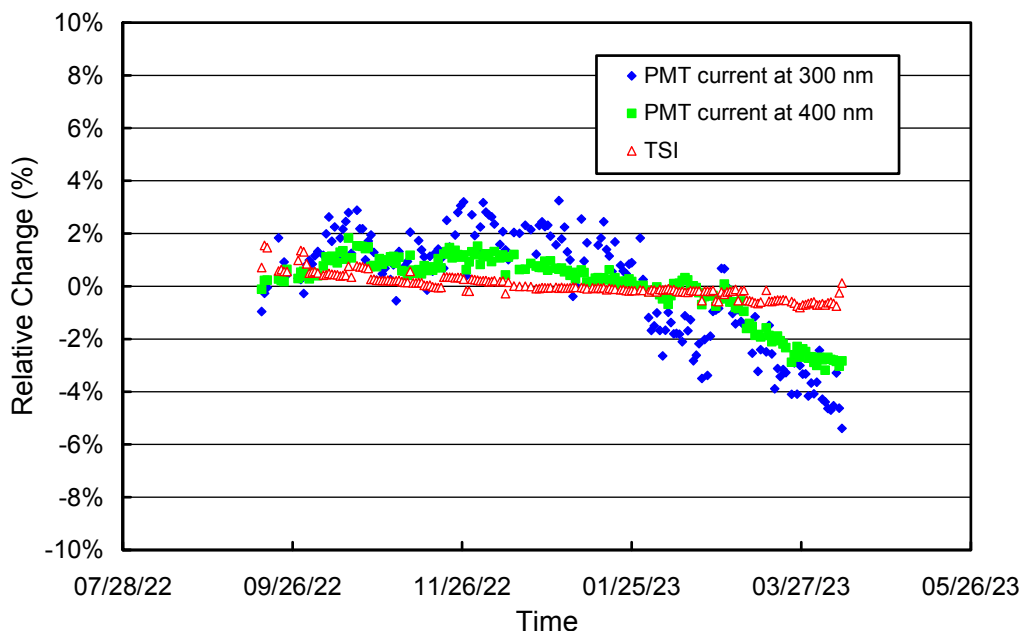


Figure 2. Time-series of PMT current at 300 and 400 nm, plus the TSI signal, derived from daily measurements of the SUV-100’s the internal irradiance standard. Data are normalized to the average of the whole period.

A comparison of GUV-541 and SUV-100 measurements allows to detect anomalies in SUV-100 data. Accordingly, Figure 3 shows the ratio of GUV-541 (340 nm channel) and SUV-100 measurements. The latter were weighted with the spectral response function of the GUV’s 340 nm channel. The ratio was normalized to its average and should ideally be equal to one at all times. The graphs indicates that GUV and SUV measurements are generally consistent to within $\pm 5\%$. The few outliers can be explained by shading from obstacles (e.g., air sampling masts) that are in the field of view of the instruments. Because GUV and SUV radiometers are not positioned at exactly the same location, the shadows from these obstacles fall on the collectors of the two instruments at different times. Scans affected by shadowing from stacks were flagged in the SUV-100 Version 2 dataset, removed from the GUV dataset, but remain part of the SUV-100 Version 0 dataset. The ratio tends to be low at the start and end of the reporting period. This bow-shaped feature is normal and caused by uncertainties in GUV data when the solar zenith angle is very low. The upper envelope of the ratio is composed of data collected during clear-sky periods while lower ratios refer to overcast conditions. (Data used for the plot are based on a preliminary cosine error correction, which is less sophisticated than that used for Version 2 SUV data. For example, it does not take the effect of clouds into account).

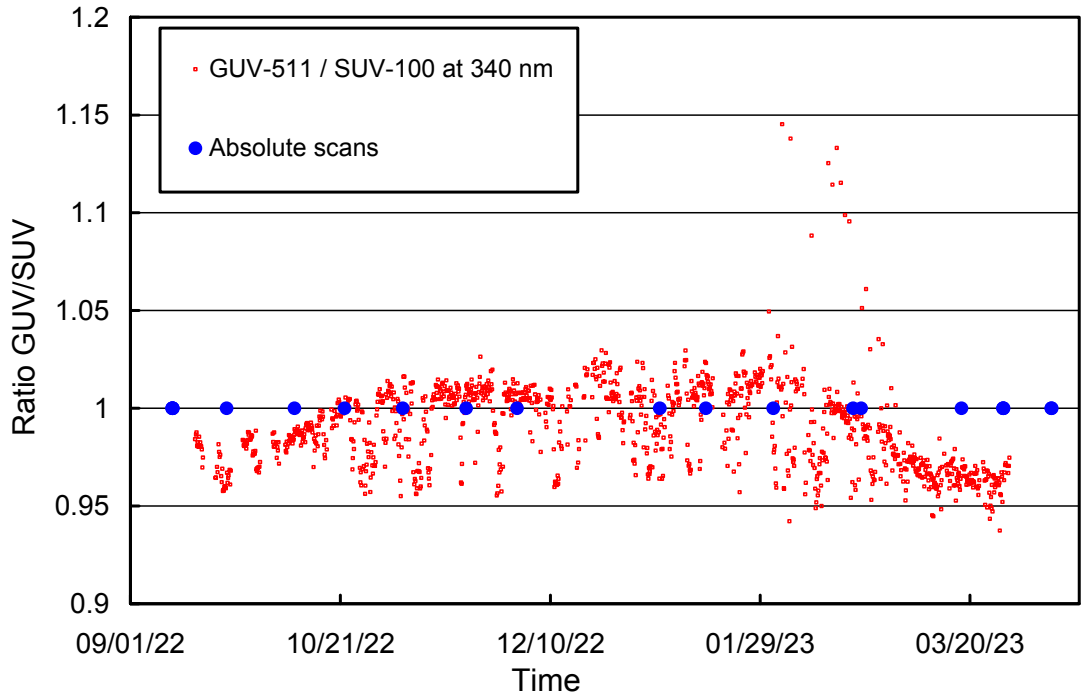


Figure 3. Ratio of GUV-541 (S/N 29239) measurements (340 nm channel) with SUV-100 measurements. SUV-100 data were weighted with the spectral response function of this GUV channel.

Figure 4 shows the ratio of all calibration scans performed during the reporting period to the average of these scans. All ratios deviate less than $\pm 1.5\%$ from the average; in the visible range, the departure is even smaller. This level of variation is similar to that shown in Figure 1. There is no clear drift in the calibration scans over time: functions determined at the start of the reporting period (shown in red and yellow colors) and those calculated at the end of the period (shown in green and blue colors) are equally distributed about the range. However, measurements with lamp M-666 (indicated by symbols with a black border) tend to be larger than measurements with lamp 200W021 (indicated by symbols with uniform color). This pattern is also similar to that shown in Figure 1, confirming the slight difference in the calibration scale of the two lamps. However, it is not possible to determine which of two lamps is closer to the truth and the difference of about 1% is part of the measurement uncertainty. All solar spectra of the reporting period were calibrated with the average of the calibration scans indicated in Figure 4.

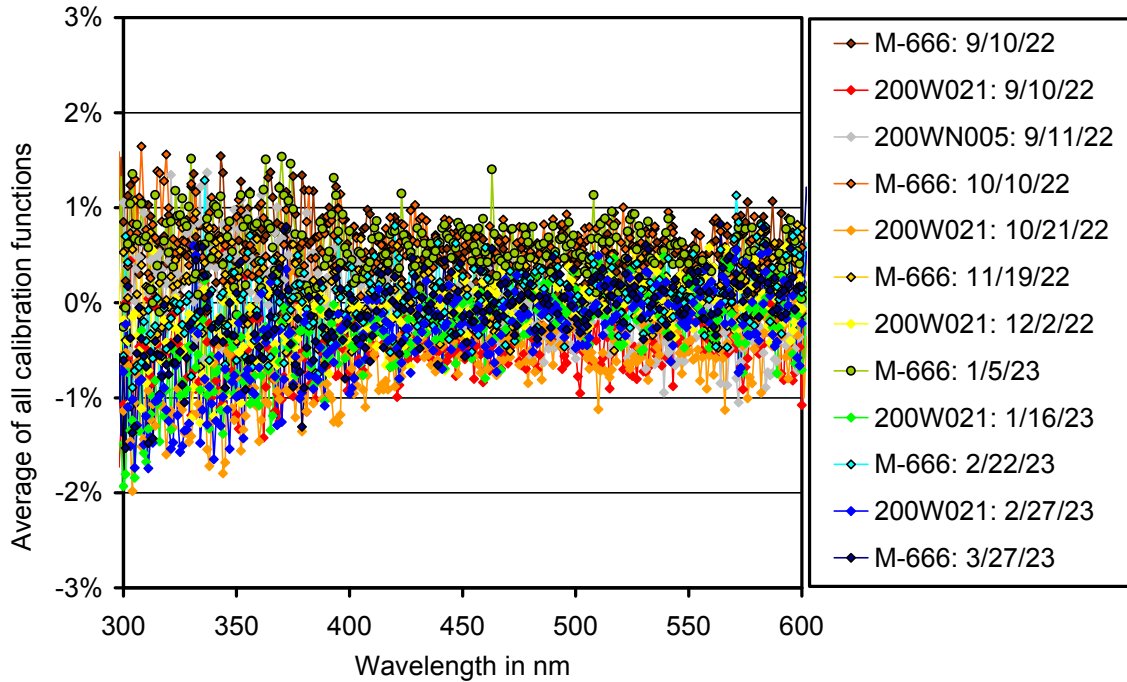


Figure 4. Ratio of calibration functions (aka “absolute scans”) performed during the reporting period and the average of these functions. The legend indicates the lamp and date of each calibrations. Measurements of lamp M-666 are indicated with symbols with a black border.

As indicated in Figure 5, the average of these calibration functions is in excellent agreement with the last calibration function of the previous reporting period (Volume 31), which was applied to solar measurements of the period 03/11/22 – 03/31/22. This confirms the good consistency of calibrations applied in the two reporting periods.

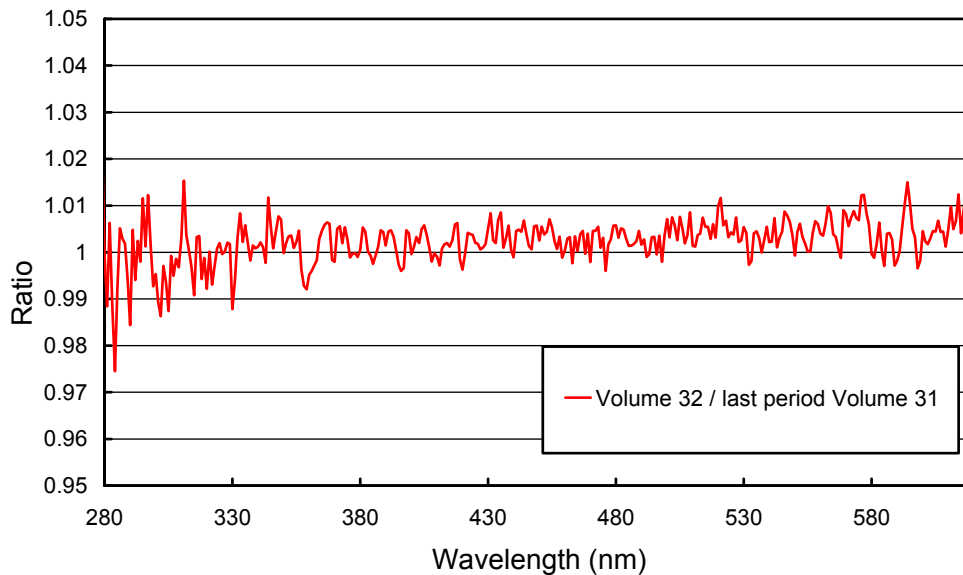


Figure 5. Ratio of the average of the calibration functions shown in Figure 4 and the last calibration function applied during the Volume 31 reporting period.

3.3. Wavelength Calibration

The wavelength stability of the system was monitored with the internal mercury lamp. Information from the daily wavelength scans was used to homogenize the dataset by correcting day-to-day fluctuations in the wavelength offset. The wavelength-dependent bias of this homogenized dataset and the correct wavelength scale was determined with the Version 2 Fraunhofer line correlation method (Bernhard et al., 2004). The resulting correction function is shown in Figure 6.

Figure 7 indicates the wavelength accuracy of Version 0 data for five wavelengths in the UV and visible range. The plot was generated by applying the Fraunhofer-line correlation method to the corrected data. Residual wavelength shifts are typically smaller than ± 0.10 nm, but there is still a noticeable day-to-day variability. Of note, some wavelengths at the very beginning of the reporting period (9/16/22 – 9/18/22) are shifted by as much as 0.3 nm (oval circle in Figure 7). During this period, the wavelength mapping function of the monochromator had a different pattern than that indicated in Figure 6.

The wavelength accuracy was further improved when processing Version 2 data by breaking the dataset into 92 periods and calculating separate correction functions for each period. This procedure also corrected the relatively large wavelength errors affecting data during the first days of the reporting period. Figure 8 indicates the wavelength accuracy of Version 2 data. A significant improvement in the wavelength uncertainty can be observed when comparing Figures 7 and 8. The standard deviation of the residual wavelength shifts indicated in Figure 8 is smaller than 0.038 nm at all wavelengths.

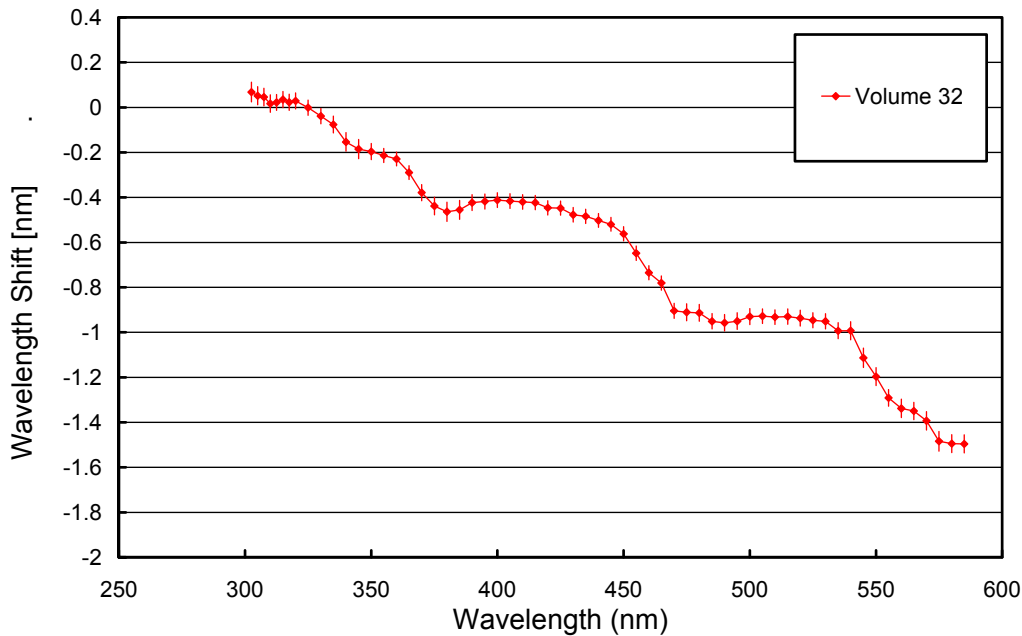


Figure 6. Monochromator non-linearity correction functions.

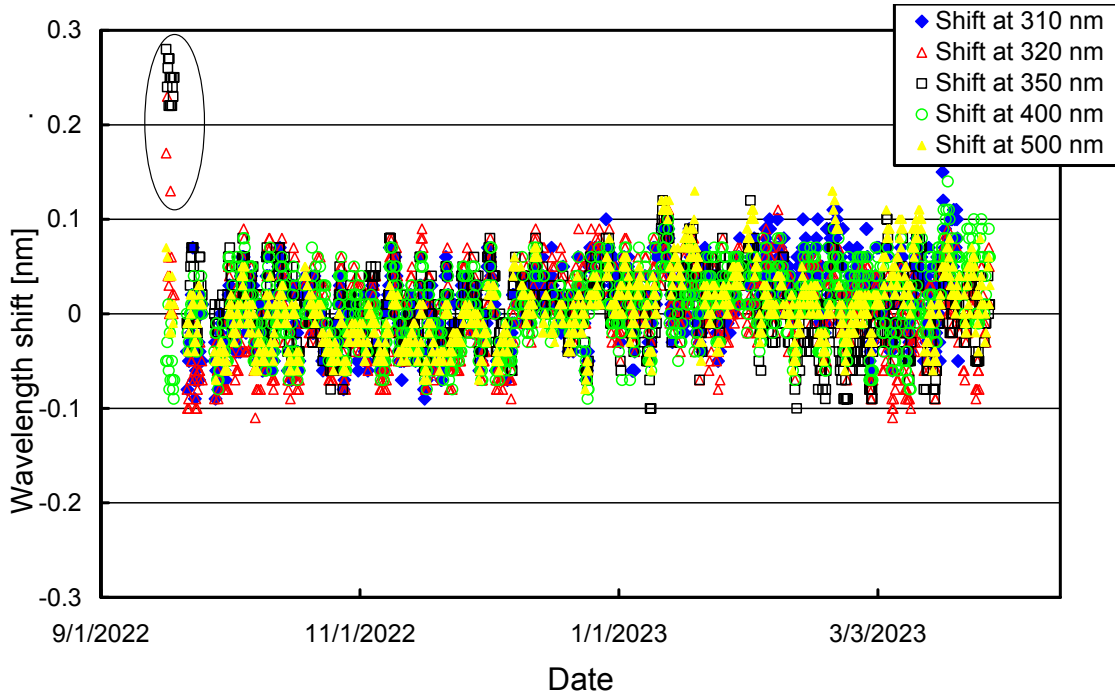


Figure 7. Wavelength accuracy check of Version 0 data at five wavelengths by means of Fraunhofer-line correlation.

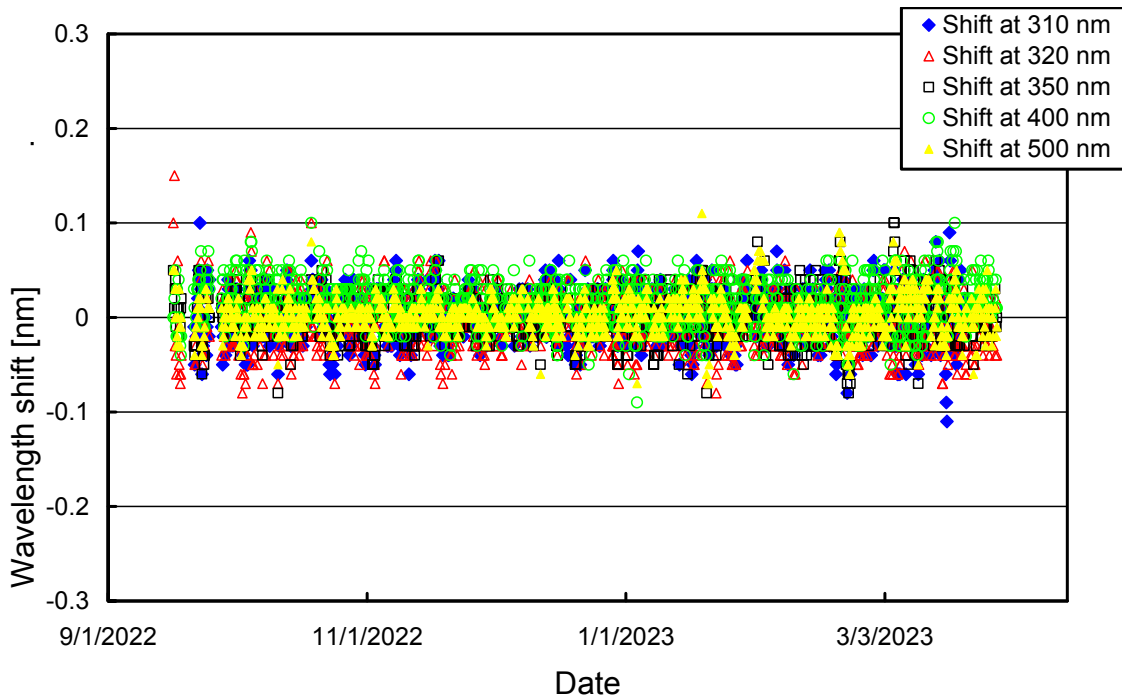


Figure 8. Wavelength accuracy check of Version 2 data at five wavelengths by means of Fraunhofer-line correlation.

3.4. Missing data

Table 1 provides a list of days that have substantial (> 12 hours) data gaps, plus indications of their causes. There were frequent problems with the communication between the computer and the unit that controls the wavelength setting of the monochromator, resulting in the monochromator's wavelength registration being either out of range or undefined. Affected data could not be processed and are therefore not part of the dataset.

Table 1: Days with substantial data gaps.

Date	Reason
09/19/22 – 09/20/22	Wavelength registration of monochromator out of range
09/25/22 – 09/27/22	Wavelength registration of monochromator out of range
10/18/22	Wavelength registration of monochromator out of range
12/17/22	Wavelength registration of monochromator out of range
12/19/22	Wavelength registration of monochromator out of range
01/06/23	Wavelength registration of monochromator out of range
01/10/23	Wavelength registration of monochromator out of range
01/30/23	Wavelength registration of monochromator out of range
03/22/23	Wavelength registration of monochromator out of range
03/28/23	Unknown

References

- Bernhard, G., C. R. Booth, and J. C. Eshamjian. (2004). Version 2 data of the National Science Foundation's Ultraviolet Radiation Monitoring Network: South Pole, *J. Geophys. Res.*, 109, D21207. <https://doi.org/10.1029/2004JD004937>
- Bernhard G. and S. Stierle (2020). Trends of UV Radiation in Antarctica, *Atmosphere*, 11(8), 795. <https://doi.org/10.3390/atmos11080795>